



# Oxygen potential of solid solution $\text{Eu}_y\text{U}_{1-y}\text{O}_{2+x}$

Takeo Fujino <sup>a,\*</sup>, Nobuaki Sato <sup>a</sup>, Kohta Yamada <sup>a</sup>, Shohei Nakama <sup>a</sup>,  
Kousaku Fukuda <sup>b</sup>, Hiroyuki Serizawa <sup>b</sup>, Tetsuo Shiratori <sup>b</sup>

<sup>a</sup> Institute for Advanced Materials Processing, Tohoku University, 2-1-1 Katahira, Aoba-ku, Sendai 980-8577, Japan

<sup>b</sup> Japan Atomic Energy Research Institute, Tokai Research Establishment, Tokai-mura, Naka-gun, Ibaraki-ken 319-1195, Japan

Received 15 April 1998; accepted 20 August 1998

---

## Abstract

The oxygen potential,  $\Delta\bar{G}_{\text{O}_2}$ , of  $\text{Eu}_y\text{U}_{1-y}\text{O}_{2+x}$  solid solution was measured as a function of  $x$  value for  $y=0.05$  and  $0.1$  at  $1000$ ,  $1100$  and  $1200^\circ\text{C}$  using an electrobalance. With the addition of europium, a significant increase in  $\Delta\bar{G}_{\text{O}_2}$  was observed in the hypostoichiometric region, but its effect was almost the same for  $y=0.05$  and  $0.1$  in the hyperstoichiometric region. The O/M ( $M=\text{Eu} + \text{U}$ ) ratio, which yields the steepest change of  $\Delta\bar{G}_{\text{O}_2}$ , decreased with decreasing temperature in the range ca.  $1000$ – $1400^\circ\text{C}$  for  $y=0.1$ , although this effect was not seen for  $y=0.05$ . The temperature dependence of this decrease seemed to be enhanced as the  $y$  value increased. Both the partial molar entropy and enthalpy of oxygen ( $\Delta\bar{S}_{\text{O}_2}$  and  $\Delta\bar{H}_{\text{O}_2}$ ) for  $y=0.1$  solid solution showed sharp large peaks at O/M ratios slightly less than  $2$ . Such peaks emerge as a result of the above decrease of the O/M ratio for steepest change of  $\Delta\bar{G}_{\text{O}_2}$ , with decreasing temperature. © 1999 Elsevier Science B.V. All rights reserved.

PACS: 28.41.Bm

---

## 1. Introduction

Uranium dioxide accommodates foreign metals, A, in the cubic fluorite type crystal forming solid solutions  $\text{A}_y\text{U}_{1-y}\text{O}_{2+x}$  ( $x \geq 0$ ). The A metals are those which take on either  $+4$ ,  $+3$  or  $+2$  valence states [1–7] in a limited range of crystal radii of  $0.6$ – $1.2$  Å (CN = 8). The thermodynamic properties of the solid solutions are largely altered with the valence of the A metals, as has been discussed in the literature [8].

The oxygen potential ( $\Delta\bar{G}_{\text{O}_2}$ ) of europium solid solution,  $\text{Eu}_y\text{U}_{1-y}\text{O}_{2+x}$ , has been measured for  $y=0.1$  and  $0.3$  at  $850$  and  $1050^\circ\text{C}$  [9,10].  $\Delta\bar{G}_{\text{O}_2}$  was seen to increase significantly by the addition of europium, which is in line with the behavior seen for the most solid solutions. However, in addition to this,  $\Delta\bar{G}_{\text{O}_2}$  of  $\text{Eu}_y\text{U}_{1-y}\text{O}_{2+x}$  was peculiar in a point that the steepest change of  $\Delta\bar{G}_{\text{O}_2}$  took place at  $x < 0$  (i.e. O/M  $< 2.0$  where  $M=\text{Eu} + \text{U}$ ). Such a negative  $x$  value is also known for  $\text{Mg}_y\text{U}_{1-y}\text{O}_{2+x}$

[7], but the  $x$  values are zero for the solid solutions with trivalent lanthanide elements [3–6,11,12]. This phenomenon was, therefore, considered to be associated with a possible  $\text{Eu}^{2+}$  state in  $\text{Eu}_y\text{U}_{1-y}\text{O}_{2+x}$  at high temperatures [9,10]. Park and Olander [13] showed it to be explicable by assuming the formation of a dopant-vacancy cluster  $(6\text{Eu}:2\text{V})''$  in combination with the oxygen-interstitial site reduction factor  $f$ . On the other hand, the same  $\Delta\bar{G}_{\text{O}_2}$  change could be interpreted by calculating the configurational entropy change in the crystal of the europium solid solution assuming the formation of two kinds of clusters of  $\text{Eu}^{2+}$  with  $\text{U}^{5+}$ , i.e.  $\text{Eu}^{2+}-\text{U}^{5+}$  and  $\text{U}^{5+}-\text{Eu}^{2+}-\text{U}^{5+}$  [14,15], these clusters being shown as (Eu:U)' and (Eu:2U) by the Kröger and Vink notation [16].

The present study was undertaken with the aim to obtain more experimental  $\Delta\bar{G}_{\text{O}_2}$  data on  $\text{Eu}_y\text{U}_{1-y}\text{O}_{2+x}$  so that closer examination of the thermodynamic properties becomes possible for this solid solution. In our earlier paper [10], the  $\text{Eu}_y\text{U}_{1-y}\text{O}_{2+x}$  sample was equilibrated with the intended oxygen partial pressure of CO/CO<sub>2</sub> mixed gas, followed by rapid cooling in vacuum. The O/M ratio corresponding to that oxygen partial

---

\* Corresponding author. Tel.: +81-22 217 5163; fax: +81-22 217 5164; e-mail: fujino@ibis.iamp.tohoku.ac.jp

pressure (and to that oxygen potential) was obtained by weight measurement of the sample at room temperature. In the present work, the weight was measured in situ using an electrobalance at temperatures of 1000, 1100 and 1200°C for the samples of  $y = 0.05$  and  $0.1$ .

## 2. Experimental

### 2.1. Materials used

Uranium metal turnings were dissolved in 6 M nitric acid, and then uranium purification was carried out using the TBP extraction method. Ammonium hydroxide was added to the solution of purified uranium nitrate in dilute nitric acid. The ammonium diuranate precipitate formed was filtered, dried and converted to  $\text{UO}_3$  by heating in air at 500°C [17]. Stoichiometric  $\text{UO}_2$  was obtained by heating the  $\text{UO}_3$  in a stream of hydrogen at 1000°C for 6 h. The main metallic impurities in  $\text{UO}_2$  as analyzed by ICP method are shown in Table 1.

Europium sesquioxide with 99.9% purity was purchased from Nippon Yttrium Co., Ltd. Hydrogen gas used (99.99999%) was produced by a Whatman Model 75-34JA-100 hydrogen generator. Carbon dioxide and nitrogen (99.99%) gases were obtained from Nippon Sanso Co., Ltd. and used as received.

### 2.2. Preparation of solid solution

The calculated weights of  $\text{UO}_2$  and  $\text{Eu}_2\text{O}_3$  were intimately mixed in an agate mortar for 40 min. The mixture was heated in air in a muffle furnace at 800°C for three days to give europium–uranium oxides in oxidized forms. The cycle of mixing and heating was repeated three times in order to have homogeneous products.

The air heated product ( $\sim 1$  g) was pressed into 10 mm  $\phi$  pellets, and heated on an alumina boat in a horizontal SiC tube furnace at 1250°C for two days in a stream of  $\text{CO}_2/\text{H}_2$  mixed gas of which the mixing ratio was controlled to 10:0.25 ml  $\text{min}^{-1}$  by two mass-flow controllers (Kofloc, Type-3510 1/4SW-500SCCM and 1/4-10 SCCM). This mixing ratio yields the oxygen partial pressure of  $7.8 \times 10^{-3}$  Pa at 1250°C. After the reaction, the product was crushed and mixed. The mixture was

heated again in the form of pellets under the same conditions. The solid solutions formed were subjected to the oxygen potential measurements after X-ray diffraction and chemical analyses.

### 2.3. X-ray diffraction analysis

X-ray powder diffractometry was carried out with a Rigaku Type RAD-IC diffractometer using  $\text{CuK}\alpha$  radiation (40 kV, 20 mA) monochromatized with curved pyrolytic graphite. The slit system used was  $1^\circ$ – $0.5$  mm– $1^\circ$ – $0.15$  mm. The measurement was made in a range  $10^\circ \leq 2\theta \leq 140^\circ$  with a scanning rate of  $1^\circ(2\theta) \text{ min}^{-1}$ . The cubic lattice parameter of the solid solutions was calculated by the least-squares method using the LCR2 program [18].

### 2.4. Chemical analysis

Ten to 20 mg of solid solution powder was weighed to an accuracy of  $\pm 10 \mu\text{g}$  and dissolved in 5 ml  $\text{Ce(IV)}$  solution in 1.5 M sulfuric acid. For the solid solution,  $\text{Eu}_y\text{U}_{1-y}\text{O}_{2+x}$ , of known  $y$  value, the  $x$  value was determined by titrating the excess  $\text{Ce(IV)}$  with standard  $\text{Fe(II)}$  ammonium sulfate solution using ferroin indicator [19,20]. The estimated standard deviation in the titrated  $x$  values by this method is  $\pm 0.005$ .

### 2.5. Oxygen potential measurement

The precisely weighed sample (400–800 mg) in quartz basket was suspended by platinum wire from a Cahn RG-type electrobalance. The whole system was evacuated with a rotary pump. After 1 h of evacuation, the stopcock connected to the rotary pump was closed, and the vacuum leak of the system if any was detected by monitoring the mercury manometer level during several hours. Nitrogen gas was slowly introduced into the system up to the ambient pressure, and then the gas was changed to the  $\text{CO}_2/\text{H}_2$  mixed gas of intended flow rate (mixing ratio). The relation between the mixing ratio and oxygen partial pressure at a fixed temperature was calculated from the  $\Delta\bar{G}_f^\circ$  values for  $\text{H}_2\text{O(g)}$ ,  $\text{CO}_2(\text{g})$  and  $\text{CO(g)}$  [21].

Subsequently, the furnace temperature was raised, and the sample was led to absorb or liberate oxygen until no weight change was recorded. After a constant weight was observed for several hours, the mixing ratio of  $\text{CO}_2/\text{H}_2$  was changed in order to give the next oxygen partial pressure at which the weight in equilibrium was then measured. Below  $p_{\text{O}_2} < 10^{-11}$  Pa, nickel wire was used instead of platinum wire to suspend the sample. After a series of measurements at various oxygen partial pressures, the sample was equilibrated to  $p_{\text{O}_2} = 10^{-8}$  Pa followed by evacuation and furnace cooling. The solid solutions generally give the nearly vertical change in the

Table 1  
Metallic impurities in  $\text{UO}_2$

Element	Amount (ppm)
Pd	54
Y	2
La	4
Tm	94
Th	4

oxygen potential versus O/M ratio curves around this oxygen partial pressure at 1000–1200°C [8]. Therefore, the O/M ratio ( $x$  value) for the oxygen partial pressures around  $p_{\text{O}_2} = 10^{-8}$  Pa can be used as a good reference point of the measurements by the electrobalance. The  $x$  value of the treated sample was determined by chemical analysis. From the weight change of the sample in a different oxygen partial pressure, as recorded by the electrobalance, the  $x$  value for that oxygen partial pressure was obtained using the above reference  $x$  value at  $p_{\text{O}_2} = 10^{-8}$  Pa.

### 3. Results and discussion

#### 3.1. Earlier data for vacuum heating at 1400°C

In our earlier work [10] it was shown that the solid solution  $\text{Eu}_y\text{U}_{1-y}\text{O}_{2+x}$  exists in a single phase for  $y$  values in a range of  $0 \leq y \leq 0.51$  under the vacuum of  $4 \times 10^{-4}$  Pa at 1400°C, though it possibly splits into two phases on slow cooling of the specimens from 1400°C if their  $y$  values are small. The above europium solubility was obtained from the lattice parameter change with  $y$ . The lattice parameter is considered to be expressed in the form  $a = 5.4704 + sy + tx$ , where  $s$  and  $t$  are the coefficients of the linear change. Then, if the relation  $x = uy$  holds, where  $u$  is the proportionality constant, the above form can be rewritten as  $a = 5.4704 + sy + tuy = 5.4704 + (s + tu)y$ . The lattice parameter in our earlier work linearly decreased with increasing  $y$  until  $y = 0.51$ , which was in good agreement with those of Grossman et al. [22] and Ohmichi et al. [23], giving an apparent relation,  $a = 5.4704 - 0.1292y$  (Å). The relation  $x = uy$ , which is necessary to express the explicit representation  $a = 5.4704 + sy + tx$  with the observed change of lattice constant, implies that the  $x$  value is virtually unaffected by the change of  $\Delta\bar{G}_{\text{O}_2}$ : This  $x$  value is exactly or at least nearly that which gives the steepest change of  $\Delta\bar{G}_{\text{O}_2}$  and is proportional to  $y$ . The  $x$  change experimentally obtained was  $x = -0.0856y$  (i.e.  $u = -0.0856$ ) for  $0 \leq y \leq 0.51$ . Thus, if the  $t$  value is assumed to be  $-0.30$  from the literature [3,18,23–25], the lattice parameter is given by  $a = 5.4704 - 0.155y - 0.30x$ . The coefficient of  $y$  in this equation,  $s = -0.155$ , is in accord with  $-0.144$  for  $\text{Eu}^{3+}$  [23]. Since the coefficient of  $y$  for  $\text{Eu}^{2+}$  is assumed to be around  $+0.02$  [8], the above experimental data support the trivalency of europium in  $\text{Eu}_y\text{U}_{1-y}\text{O}_{2+x}$ , which is consistent with the result of Mössbauer spectroscopy [26]. It should be noted, however, that the lattice parameter and the Mössbauer peak measurements were carried out at room temperature or liquid helium temperature for the specimens which had been heated at 1400°C. That is to say, it is possible that europium is divalent at the higher temperatures (850–1200°C) of the oxygen potential

measurements. With the rise of temperature, a part of the  $\text{Eu}^{3+}$  ions in the crystal change to  $\text{Eu}^{2+}$ , while the corresponding amount of  $\text{U}^{4+}$  ions are oxidized to  $\text{U}^{5+}$ .

The oxygen potential of  $\text{Eu}_y\text{U}_{1-y}\text{O}_{2+x}$  as a function of O/M ratio shows a steepest change at O/M  $< 2.0$  [9,10], although the change position is 2.0 for  $\text{A}_y\text{U}_{1-y}\text{O}_{2+x}$  solid solutions with trivalent or tetravalent A metals. This difference has been explained assuming the cluster formation of  $\text{Eu}^{2+}$  with oxygen vacancy and/or  $\text{U}^{5+}$  [13–15].

Since the above heating experiments were carried out in a vacuum of  $4 \times 10^{-4}$  Pa ( $p_{\text{O}_2} \cong (4/5) \times 10^{-4} = 8 \times 10^{-5}$  Pa) at 1400°C, the equilibrium  $\Delta\bar{G}_{\text{O}_2}$  value becomes ca.  $-290$  kJ/mol. As has been discussed above, with this  $\Delta\bar{G}_{\text{O}_2}$  value the O/M ratios which give the steepest changes of  $\Delta\bar{G}_{\text{O}_2}$  will be obtained. Such O/M ratios at 1400°C are given as 1.996, 1.991 and 1.974 for  $y = 0.05$ , 0.1 and 0.3, respectively, by the relation  $x = -0.0856y$ .

To give a thermodynamic background for the assumption that the  $\text{Eu}^{2+}$  ions increasingly emerge with the increase of temperature, let us consider a crude model that the  $\text{Eu}^{2+}$ ,  $\text{Eu}^{3+}$ ,  $\text{U}^{4+}$  and  $\text{U}^{5+}$  ions statistically occupy the metal sites of the  $\text{UO}_2$  fluorite type crystal. Here, the cluster formation between such cations, which should be the second effect, is not taken into account. The solid solution is expressed as  $\text{Eu}_p^{2+}\text{Eu}_{y-p}^{3+}\text{U}_q^{4+}\text{U}_{1-y-q}^{5+}\text{O}_{2+x}^{2-}$  ( $x \leq 0$ ). The  $p$  and  $q$  in the above formula are:

$$p = \frac{m}{m+1}y, \quad (1)$$

$$q = 1 - 2y - 2x - \frac{m}{m+1}y, \quad (2)$$

where  $m$  is the ratio of the  $\text{Eu}^{2+}$  and  $\text{Eu}^{3+}$  ions. The number of ways of arranging the  $\text{Eu}^{2+}$ ,  $\text{Eu}^{3+}$ ,  $\text{U}^{4+}$  and  $\text{U}^{5+}$  ions over the  $N$  (= Avogadro's number) lattice sites will be

$$W = \frac{N!}{(pN)!\{(y-p)N\}!(qN)!\{(1-y-q)N\}!}. \quad (3)$$

The configurational entropy,  $\Delta S = k \ln W$ , is obtained using Eqs. (1) and (2) as:

$$\Delta S = R \left\{ \frac{-my}{m+1} \ln \left( \frac{my}{m+1} \right) - \frac{y}{m+1} \ln \left( \frac{y}{m+1} \right) - f(y, x, m) \ln f(y, x, m) - g(y, x, m) \ln g(y, x, m) \right\}, \quad (4)$$

where  $R$  is the gas constant and

$$f(y, x, m) = y + 2x + \frac{m}{m+1}y, \quad (5)$$

$$g(y, x, m) = 1 - 2y - 2x - \frac{m}{m+1}y. \quad (6)$$

Using Eq. (4), the contribution of the configurational entropy to the free energy change,  $-T\Delta S$ , was calculated for a case  $y=0.1$  and  $T=1273$  K. The solid, dash-dotted and broken lines in Fig. 1 show the variation of  $-T\Delta S$  with O/M ratio for  $m \rightarrow \infty$  (only  $\text{Eu}^{2+}$  ions),  $m=1$  ( $\text{Eu}^{2+}:\text{Eu}^{3+}=1:1$ ) and  $m \rightarrow 0$  (only  $\text{Eu}^{3+}$  ions), respectively. It is seen from the figure that the solid line is lower than the broken line by, for example, 1.9 and 2.4  $\text{kJ mol}^{-1}$  at O/M = 1.99 and 1.97, respectively. The above result suggests that the  $\text{Eu}^{2+}$  state is more favorable than the  $\text{Eu}^{3+}$  state at higher temperatures. Since  $-T\Delta S$  is a linear function of absolute temperature, the configurational effect is much smaller at room temperature or liquid helium temperature possibly causing the dominant presence of  $\text{Eu}^{3+}$  ions at low temperatures.

### 3.2. O/M ratio for the steepest $\Delta\bar{G}_{\text{O}_2}$ change as a function of temperature

The O/M ratio for an intended  $\Delta\bar{G}_{\text{O}_2}$  value was obtained by measuring the weight change on the recorder of the electrobalance. If no further weight change was observed during several hours of holding at a constant temperature, this weight was regarded as the one which

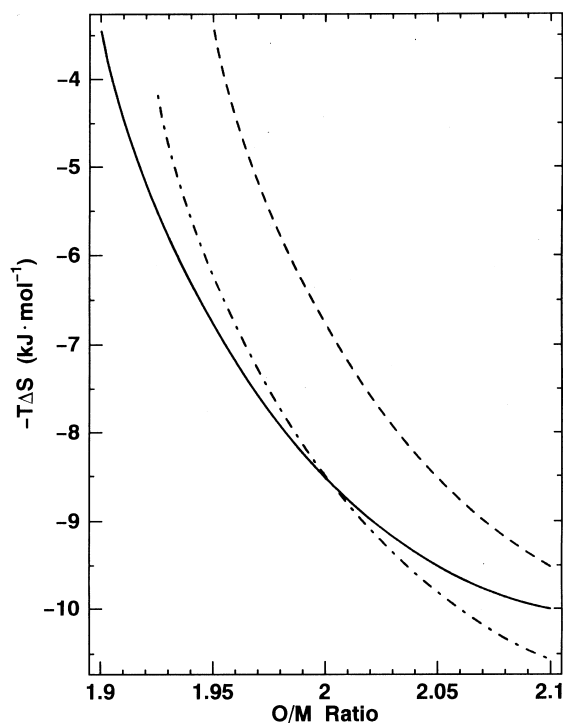


Fig. 1. Contribution of configurational entropy of cation arrangement to the change of free energy,  $-T\Delta S$ , as a function of O/M ratio.  $y=0.1$ , Temperature:  $1000^\circ\text{C}$ , Solid line:  $\text{Eu}^{2+}/\text{Eu}^{3+}=\infty$ , Dash-dotted line:  $\text{Eu}^{2+}/\text{Eu}^{3+}=1$ , Broken line:  $\text{Eu}^{2+}/\text{Eu}^{3+}=0$ .

was in equilibrium with that oxygen partial pressure. The next measurement was made by keeping the sample in the different oxygen partial pressure (and thus different  $\Delta\bar{G}_{\text{O}_2}$ ). However, it was seen that the direction of the oxygen partial pressure change affects the rate of the equilibrium attainment as shown in Fig. 2. In the figure, curve 1 indicates the variation of O/M ratio for  $\text{Eu}_{0.05}\text{U}_{0.95}\text{O}_{2+x}$  at  $1200^\circ\text{C}$  when  $\Delta\bar{G}_{\text{O}_2}$  was changed from higher to lower values. Curve 2 shows the variation of the O/M ratio when the  $\Delta\bar{G}_{\text{O}_2}$  value was changed in the opposite direction. There is a fairly large difference in these two curves. Because of the fluctuation of the baseline, the long time heating of the sample in the electrobalance did not always give good results. In order to know which curve represents the change in equilibrium, a series of experiments were performed where the sample solid solution was heated in a stream of the mixed gas for a sufficiently long period of 2–3 days. Then, after the sample was quenched to room temperature in vacuum, its composition was determined by chemical analysis. The result showed that the equilibrium curve was close to curve 1, suggesting that the solid solution oxides attain equilibrium more easily by liberating oxygen than by absorbing it from low pressure  $p_{\text{O}_2}$  atmospheres.

The O/M ratio for the steepest  $\Delta\bar{G}_{\text{O}_2}$  change was measured by the same method: The solid solution was kept at respective temperatures of 1000, 1100 and

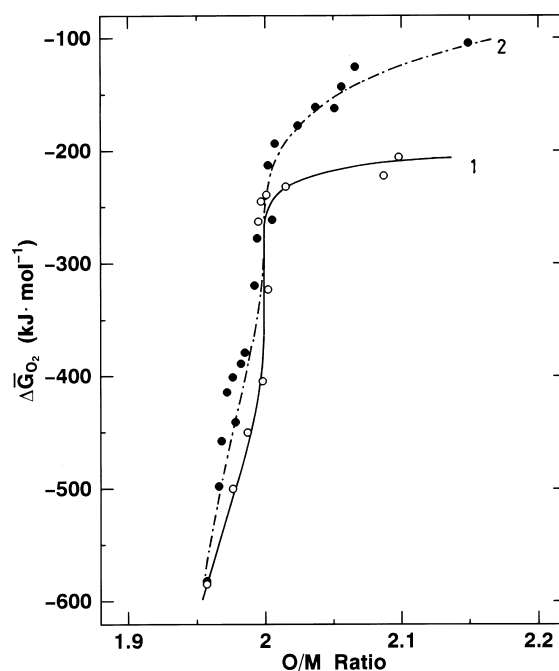
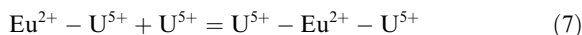


Fig. 2. Oxygen potential curves for  $\text{Eu}_{0.05}\text{U}_{0.95}\text{O}_{2+x}$  showing the effect of the direction of O/M ratio change. Temperature:  $1200^\circ\text{C}$ , Curve 1 (—, ○): Decreasing O/M ratio, Curve 2 (---, ●): Increasing O/M ratio.

1200°C in an atmosphere of  $p_{\text{O}_2} \cong 10^{-8}$  Pa for three days. The measurements at 1100°C were made only for this purpose. The equilibrated sample was cooled in vacuum followed by determination of the O/M ratio by chemical analysis.

The square marks in Fig. 3 indicate the obtained O/M ratios for  $y = 0.05$ . The filled marks in the figure show the data from the literature [10]. It was found that the O/M ratio for  $y = 0.05$  is around 1.995 and the value does not vary with temperature in a whole range 1000–1400°C. On the other hand for  $y = 0.1$  (triangle marks), the O/M ratio slightly increases with increasing temperature from 1.987 at 1000°C to 1.991 at 1400°C. Both the literature values for  $y = 0.05$  and 0.1 at 1400°C are seen to be consistent with the present values constituting the straight lines. The temperature dependence of the O/M ratio is much larger for the solid solution with high concentration of europium,  $y = 0.3$ , as shown by the filled circles. The literature values for  $\text{Eu}_{0.3}\text{U}_{0.7}\text{O}_{2+x}$  exhibit a large increase of the O/M ratio from 1.947 for 1000°C to 1.974 for 1400°C. Between 850°C and 1050°C, however, the O/M ratio has not been observed to vary with temperature for both  $y = 0.1$  and 0.3 [10]. Therefore, the change of the above O/M ratio could be the behavior characteristic of the temperatures higher than about 1000°C.

In our earlier work [14,15], it was postulated that the reaction to form a cation complex



occurred in  $\text{Eu}_y\text{U}_{1-y}\text{O}_{2+x}$  solid solution with not very large equilibrium constant,  $K$ . If  $\alpha$  is defined as the average number of the  $\text{U}^{5+}$  ions which combine with one  $\text{Eu}^{2+}$  ion, the  $x$  value which yields the steepest  $\Delta\bar{G}_{\text{O}_2}$  change was expected to be expressed as  $x = -(1 - \alpha/2)y$ . From the observed O/M ratios obtained in this work,

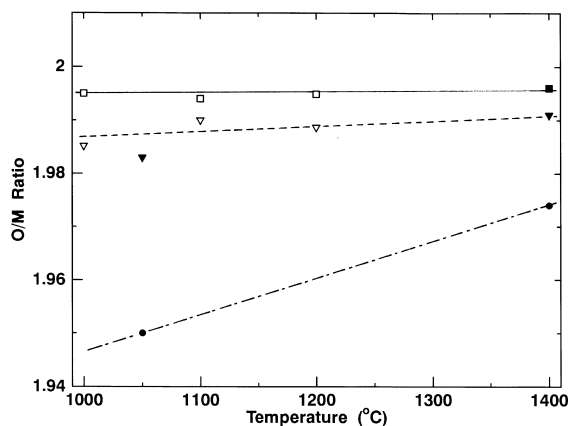


Fig. 3. O/M ratio for the steepest change of  $\Delta\bar{G}_{\text{O}_2}$  as a function of temperature.  $\square$  and  $\blacksquare$ :  $y = 0.05$ ,  $\nabla$  and  $\blacktriangledown$ :  $y = 0.1$ ,  $\bullet$ :  $y = 0.3$ . Filled marks show the data from Ref. [10].

the  $\alpha$  values can be evaluated. For  $y = 0.05$ , the value becomes  $\alpha = 1.80$  at 1000–1400°C from the data of Fig. 3. For  $y = 0.1$ , the  $\alpha$  value is 1.74 at 1000°C, whereas it increases to  $\alpha = 1.82$  at 1400°C. Such an increase can be interpreted as showing the increased possibility of formation of the  $\text{U}^{5+}-\text{Eu}^{2+}-\text{U}^{5+}$  complexes as the temperature rises giving larger  $K$  of reaction (7). It may be assumed that there are two regions of temperature with regard to the formation and decomposition of the complexes. The temperature range of 1000–1400°C in the present case is regarded as that of complex formation where  $\partial K/\partial T > 0$ , i.e.  $\Delta H^\circ > 0$  ( $\Delta H^\circ$  is assumed to be temperature independent). Thus, if the free energy of reaction (7) is negative,  $T\Delta S^\circ$  should be greater than  $\Delta H^\circ$  in this temperature range. On the other hand, the increase of the above  $\alpha$  value is also explicable in another way that  $\text{Eu}^{3+}$  ions change to  $\text{Eu}^{2+}$  ions to a larger extent with increasing temperature: The concentration of  $\text{U}^{5+}$  increases as that of  $\text{Eu}^{2+}$  increases, which causes a shift in the equilibrium of reaction (7) to the right side. The point which is the actual case is not clear at present.

### 3.3. Oxygen potential as a function of O/M ratio

Fig. 4 compares the oxygen potential at 1000 and 1200°C for  $y = 0.05$  solid solution. Curves 1 and 2 are those for 1000 and 1200°C, respectively. It is seen from the figure that the steepest  $\Delta\bar{G}_{\text{O}_2}$  change occurs at the

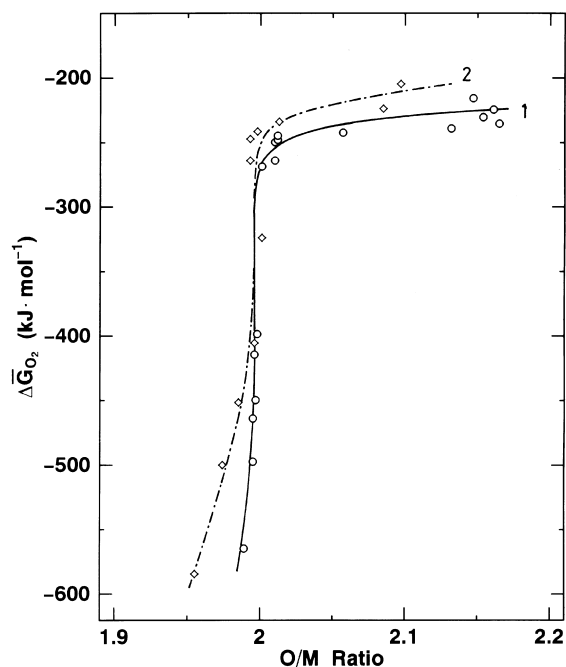


Fig. 4. Oxygen potential for  $y = 0.05$  solid solution as a function of O/M ratio. Curve 1 (—,  $\circ$ ): 1000°C, Curve 2 (---,  $\diamond$ ): 1200°C.

same O/M ratio of 1.995 for both these curves but the oxygen potential at 1200°C is higher than that at 1000°C for the O/M ratios higher and lower than 1.995. The 1200°C curve gives a slope which is not so steep as the 1000°C curve in a range of the O/M ratios below the O/M ratio for the steepest  $\Delta\bar{G}_{O_2}$  change. The O/M ratio drops to a value as small as 1.95 yielding  $\Delta\bar{G}_{O_2} = -600$  kJ mol<sup>-1</sup> at that O/M ratio.

Fig. 5 shows the oxygen potential for  $y = 0.1$  solid solution. Curves 1 and 2 indicate the variation of  $\Delta\bar{G}_{O_2}$  at 1000 and 1200°C, respectively. As has been stated in Section 3.2., the O/M ratio for the steepest  $\Delta\bar{G}_{O_2}$  change increases with increasing temperature for this europium concentration. The slope of the curves below those O/M ratios becomes smaller as the O/M ratio is lowered. The oxygen potential of  $-550$  kJ mol<sup>-1</sup> is obtained at O/M = 1.95 (1000°C). This  $\Delta\bar{G}_{O_2}$  value is higher than that of 1200°C by about 50 kJ mol<sup>-1</sup> as a result of lower slope of the 1000°C curve. Above the O/M ratios for the steepest  $\Delta\bar{G}_{O_2}$  change, the curves of  $y = 0.1$  specimens level off more rapidly with the O/M increase than those of  $y = 0.05$ . Consequently, the  $\Delta\bar{G}_{O_2}$  value of  $y = 0.1$  is only slightly higher than that of  $y = 0.05$  in the hyperstoichiometric region at both temperatures of 1000 and 1200°C. Our earlier measurement for Eu<sub>0.1</sub>U<sub>0.9</sub>O<sub>2+x</sub> at 1050°C [10] yielded somewhat higher  $\Delta\bar{G}_{O_2}$  values in the hyperstoichiometric region. It may be because of the difference in the method of the O/M measurement. The

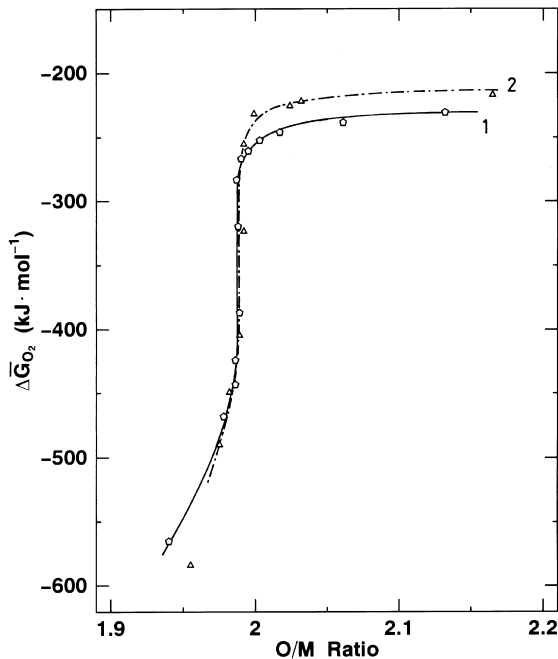


Fig. 5. Oxygen potential for  $y = 0.1$  solid solution as a function of O/M ratio. Curve 1 (—,  $\circ$ ): 1000°C, Curve 2 (- - -,  $\Delta$ ): 1200°C.

present data are thought to be more reliable considering the possible error in the obtained O/M ratios.

### 3.4. Partial molar entropy and enthalpy of oxygen as a function of O/M ratio

If it is assumed that partial molar entropy of oxygen ( $\Delta\bar{S}_{O_2}$ ) and enthalpy ( $\Delta\bar{H}_{O_2}$ ) are not functions of temperature, which is not exactly true but in many cases is roughly correct, the  $\Delta\bar{S}_{O_2}$  value can be obtained from the  $\Delta\bar{G}_{O_2}$  data for 1000 and 1200°C using the relation  $\Delta\bar{S}_{O_2} = -\partial\Delta\bar{G}_{O_2}/\partial T$ . Fig. 6 shows the  $\Delta\bar{S}_{O_2}$  change as a function of O/M ratio. Curves 1 and 2 express the  $\Delta\bar{S}_{O_2}$  change for  $y = 0.05$  and 0.1, respectively. The curve for  $y = 0.05$  increases rapidly at O/M = 1.995 with increasing O/M ratio. It then turns into a very slow decrease above O/M = 2.025 on further increase of the O/M ratio. On the other hand, the  $\Delta\bar{S}_{O_2}$  curve for  $y = 0.1$  has a sharp large peak at O/M = 1.988. This peak is undoubtedly caused from the increase of the O/M ratio with temperature. The peak position is slightly shifted from the O/M ratio for the steepest  $\Delta\bar{G}_{O_2}$  change, because  $\Delta\bar{S}_{O_2}$  was calculated from the difference of  $\Delta\bar{G}_{O_2}$  at 1200 and 1000°C. Above O/M  $\approx 2.0$ , the curve for  $y = 0.1$  is nearly horizontal.

Fig. 7 shows the partial molar enthalpy of oxygen against the O/M ratio. Curves 1 and 2 depict the variation of  $\Delta\bar{H}_{O_2}$  for  $y = 0.05$  and 0.1, respectively. From this figure it is seen that the shapes of the  $\Delta\bar{H}_{O_2}$  curves

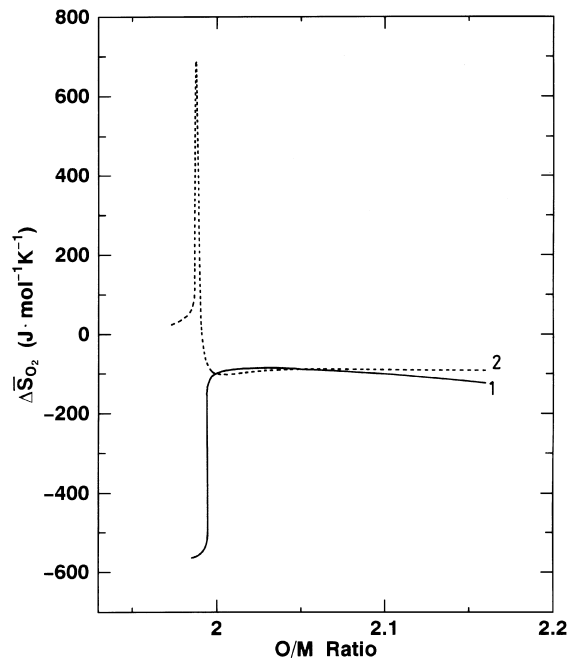


Fig. 6. Partial molar entropy of oxygen as a function of O/M ratio. Curve 1 (—):  $y = 0.05$ , Curve 2 (- - -):  $y = 0.1$ .

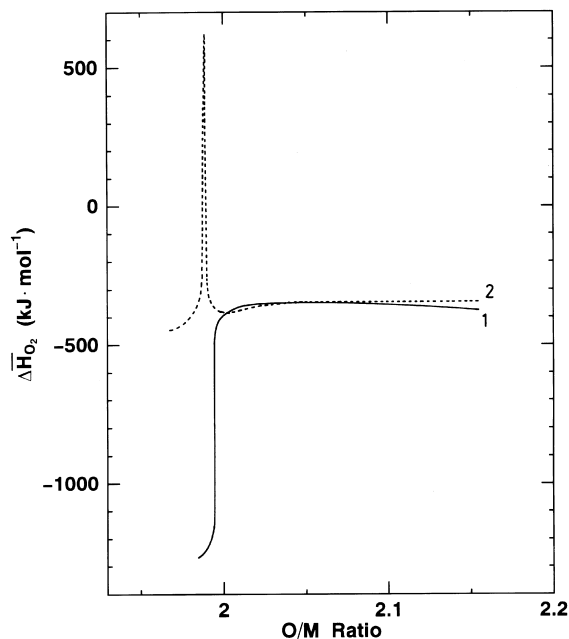


Fig. 7. Partial molar enthalpy of oxygen as a function of O/M ratio. Curve 1 (—):  $y=0.05$ , Curve 2 (- - -):  $y=0.1$ .

are similar to those of the  $\Delta\bar{S}_{O_2}$  curves (Fig. 6). Evaluation of the  $\Delta\bar{S}_{O_2}$  and  $\Delta\bar{H}_{O_2}$  values has also been carried out in our earlier work [10] for  $y=0.1$  and  $0.3$ , where the  $\Delta\bar{S}_{O_2}$  and  $\Delta\bar{H}_{O_2}$  curves showed peaks but they were broad and the peak positions were in a range of considerable hypostoichiometry. These results are not in good agreement with the present results; the main reason may be the different temperatures of measurements in the former work (850–1050°C).

The sharp peaks in the  $\Delta\bar{S}_{O_2}$  and/or  $\Delta\bar{H}_{O_2}$  curves have also been observed for other solid solutions. It has been reported that there were the sharp maxima in both  $\Delta\bar{S}_{O_2}$  and  $\Delta\bar{H}_{O_2}$  curves for  $Gd_{0.1}U_{0.9}O_{2+x}$  in the hypostoichiometric region near  $x=0$  [27,28]. A similar sharp peak of  $\Delta\bar{S}_{O_2}$  has been seen for  $Mg_{0.05}U_{0.95}O_{2+x}$  in the slight hypostoichiometry [7]. The  $\Delta\bar{S}_{O_2}$  peak of the latter solid solution is likely to have a closely related origin to that of the present  $Eu_{0.1}U_{0.9}O_{2+x}$  solid solution (i.e.  $U^{5+}-Eu^{2+}-U^{5+}$  complex formation) since magnesium is

divalent and both the two peaks appear in a hypostoichiometric region.

## References

- [1] S. Aronson, J.C. Clayton, *J. Chem. Phys.* 32 (1960) 749.
- [2] R.E. Woodley, *J. Nucl. Mater.* 96 (1981) 5.
- [3] D.I.R. Norris, P. Kay, *J. Nucl. Mater.* 116 (1983) 184.
- [4] K. Hagemark, M. Broli, *J. Am. Ceram. Soc.* 50 (1967) 563.
- [5] K. Une, M. Oguma, *J. Nucl. Mater.* 115 (1983) 84.
- [6] T.B. Lindemer, J. Brynstad, *J. Am. Ceram. Soc.* 69 (1986) 867.
- [7] J. Tateno, T. Fujino, H. Tagawa, *J. Solid State Chem.* 30 (1979) 265.
- [8] T. Fujino, C. Miyake, in: A.J. Freeman, C. Keller (Eds.), *Handbook on the Physics and Chemistry of the Actinides*, vol. 6, North-Holland, Amsterdam, 1991.
- [9] T. Fujino, *J. Nucl. Mater.* 154 (1988) 14.
- [10] T. Fujino, K. Ouchi, Y. Mozumi, R. Ueda, H. Tagawa, *J. Nucl. Mater.* 174 (1990) 92.
- [11] T. Matsui, K. Naito, *J. Nucl. Mater.* 138 (1986) 19.
- [12] J.F. Wadier, CEA-R-4507 (1973).
- [13] K. Park, D.R. Olander, *J. Nucl. Mater.* 187 (1992) 89.
- [14] T. Fujino, N. Sato, *J. Nucl. Mater.* 189 (1992) 103.
- [15] T. Fujino, N. Sato, K. Yamada, *J. Nucl. Mater.* 223 (1995) 6.
- [16] F.A. Kröger, H.J. Vink, *Solid State Physics* 3 (1956) 588.
- [17] H.R. Hoekstra, S. Siegel, E.X. Gallagher, *J. Inorg. Nucl. Chem.* 32 (1970) 3237.
- [18] D.E. Williams, Ames Lab. Rep. IS-1052 (1964).
- [19] S.R. Dharwadkar, M.S. Chandrasekharaiah, *Anal. Chim. Acta* 45 (1969) 545.
- [20] T. Fujino, T. Yamashita, *Fresenius' Z. Anal. Chem.* 314 (1983) 156.
- [21] Database MALT2, Japan Thermo-Measurement Soc. (1987).
- [22] L.N. Grossman, J.E. Lewis, D.M. Rooney, *J. Nucl. Mater.* 21 (1967) 302.
- [23] T. Ohmichi, S. Fukushima, A. Maeda, H. Watanabe, *J. Nucl. Mater.* 102 (1981) 40.
- [24] D.C. Hill, J.H. Handwerk, R.J. Beals, ANL-6711 (1963).
- [25] T. Yamashita, T. Fujino, H. Tagawa, *J. Nucl. Mater.* 132 (1985) 192.
- [26] T. Tsuji, private communication.
- [27] K. Une, M. Oguma, *J. Nucl. Mater.* 110 (1982) 215.
- [28] T.B. Lindemer, A.L. Sutton, Jr., *J. Am. Ceram. Soc.* 71 (1988) 553.